Journal of Microbiology (2022) Vol. 60, No. 10, pp. 1007–1020
DOI 10.1007/s12275-022-2173-1
eISSN 1976-3794
pISSN 1225-8873

Genomic and physiological analysis of C_{50} carotenoid-producing novel *Halorubrum ruber* sp. nov.[§]

Chi Young Hwang[1†], Eui-Sang Cho[1†], Won Jong Rhee[1,2,3], Eunjung Kim[1,2,3], and Myung-Ji Seo[1,2,3*]

[1]*Department of Bioengineering and Nano-Bioengineering, Incheon National University, Incheon 22012, Republic of Korea*
[2]*Division of Bioengineering, Incheon National University, Incheon 22012, Republic of Korea*
[3]*Research Center for Bio Materials & Process Development, Incheon National University, Incheon 22012, Republic of Korea*

(Received Apr 20, 2022 / Revised Jul 20, 2022 / Accepted Aug 9, 2022)

A novel haloarchaeal species designated as MBLA0099^T was isolated from seawater near Yeongheung Island. Cells were Gram-negative, non-motile, red-pigmented, and rod-shaped. They grew at 10–45°C, within pH 5.5–9.0, and between 7.5% and 30% NaCl concentrations. Cells were able to grow without Mg^{2+} and were lysed in distilled water. The size of the whole-genome and G + C content of DNA was 3.02 Mb and 68.9 mol%, respectively. Phylogenetic analysis shows that the strain MBLA0099^T belongs to the genus *Halorubrum*. The average nucleotide and amino acid identity, and *in silico* DNA-DNA hybridization values were below the species delineation threshold. Pan-genomic analysis revealed that 3.2% of all genes present in strain MBLA0099^T were unique to the strain. The red carotenoid produced by strain MBLA0099^T was subjected to spectrometric and chromatographic analyses and confirmed to be bacterioruberin as C_{50} carotenoid. Mevalonic acid, terpenoid backbone, and carotenoid biosynthesis pathway were annotated for strain MBLA0099^T. The C_{50} carotenoid production by strain MBLA0099^T was also enhanced under various stress conditions including relatively netural pH, high oxidative and salinity conditions. Additionally, the strain MBLA0099^T-derived bacterioruberin showed the antioxidant activity with EC_{50} value of 12.29 μg/ml, based on the evaluation of DPPH free radical scavenging activity. The present study would be the first report on the identification of C_{50} carotenoid from the strain MBLA0099^T representing a novel species of the genus *Halorubrum*, for which the name *Halorubrum ruber* sp. nov. is proposed. The type-strain used was MBLA0099^T (= KCTC 4296^T = JCM 34701^T).

***Keywords*:** haloarchaea, *Halorubrum*, isolation, carotenoid, bacterioruberin

Introduction

Members of the type-genus *Halorubrum* (*Hrr.*), belonging to the family *Halorubraceae* are widely distributed in various hypersaline environments such as marine salterns, soda lakes, salt lakes, saline soils, salt-fermented foods, and salt-preserved food products (McGenitv and Grant, 1995; Fullmer *et al.*, 2014; Gibtan *et al.*, 2018; Serrano *et al.*, 2021). Currently (end of April 2022), the genus *Halorubrum* is one of the largest groups in the family *Halorubraceae*. A total of 42 reported species may have undergone a period of rapid evolution (LPSN, https://www.bacterio.net). They are typically aerobic and chemoorganotrophic microbes that use various substrates, such as amino acids, organic acids, and sugars as carbon and energy sources (Gonzalez *et al.*, 1978; McGenitv and Grant, 1995). Colony color ranges from pink to red owing to the presence of red pigments. Species of the genus *Halorubrum* can grow between 2.9% and 30.4% (w/v) NaCl concentrations at temperatures of 30–50°C and are neutrophilic (Kamekura *et al.*, 1997). The major polar lipid profiles *Halorubrum* species consist of phosphatidylglycerol (PG), phosphatidylglycerol phosphate methyl ester (PGP-Me), phosphatidylglycerol sulfate (PGS), or glycolipids such as sulfated mannosyl glucosyl diether (S-DGD-1), depending on the species (McGenitv and Grant, 1995). Although phenotypic and chemotaxonomic analyses are widely known, genomic analyses of the taxonomic relationships among *Halorubrum* species are insufficient.

Carotenoids are derivatives of isoprenoids that originate from the terpenoid biosynthetic pathway and play diverse roles in nature. Many food materials, such as fruits, vegetables, and shellfish, are yellow, orange, or red owing to carotenoids. C_{30}, C_{40}, and C_{50} carotenoids are categorized by the number of carbons in the carotenoid skeleton (number of isoprene units) (Nakano and Wiegertjes, 2020). C_{40} carotenoids have received most of the attention in the research and development of carotenoid production technologies as their commercial value increases and interest. Several microorganisms have been proposed as renewable and efficient producers for carotenoid overproduction. In that respect, microalgae have been studied the most widely to produce carotenoids (Forján *et al.*, 2015).

C_{50} carotenoids have high potent antioxidant activity than other C_{40} carotenoids because of owing to the more conjugated double bonds in structure (Giani *et al.*, 2019; Flores *et al.*, 2020). They represent only a small proportion of these

[†]These authors contributed equally to this work.
*For correspondence. E-mail: mjseo@inu.ac.kr; Tel.: +82-32-835-8267; Fax: +82-32-835-0804
[§]Supplemental material for this article may be found at https://doi.org/10.1007/s12275-022-2173-1.

natural pigments and have been isolated from only a few microorganisms. After first report of decaprenoxanthin as C_{50} carotenoid from *Flavobacterium dehydrogenas* (Liaaen-Jensen *et al.*, 1968), several studies have been reported regarding C_{50} carotenoid-producing microorganisms, which has been however limited to haloarchaea. In addition, almost studies have just focused on the isolation of novel haloarchaea and the simple investigation of its pigment productions, with no further identification, stress-induced production, and the biological activities of the corresponding pigments.

Only a few studies have been paid to the application of bacterioruberin and the potential of haloarchaea as carotenoid producers. Most haloarchaea are bright red-orange because of the large amounts of C_{50} carotenoid pigments in the membrane (Oren and Rodriguez-Valera, 2001). Carotenoids in the archaeal cellular membrane may support cells in adapting to hypersaline environments by functioning as a water barrier and allowing ions and oxygen molecules to move into the cell membrane (Shahmohammadi *et al.*, 1998). Therefore, it is attractive to investigate carotenoid production of haloarchaea according to their ability to synthesize and accumulate both C_{40} and C_{50} carotenoids natively.

In this study, one novel strain MBLA0099^T was isolated from seawater near Yeongheung Island. Genome-based taxonomic and phylogenetic relationships between strain MBLA0099^T and other previously reported species of the genus *Halorubrum* are described. In addition, this study is focused on the C_{50} carotenoid biosynthesis based on the genome information of the isolated strain MBLA0099^T and the production profiling of bacterioruberin as C_{50} carotenoid targeted in this study. The antioxidant activity of the MBLA0099^T-derived bacterioruberin was also evaluated to propose the potential of bacterioruberin as natural antioxidant bioresource. The isolate was classified as a novel species of the genus *Halorubrum*, for which we propose the name *Halorubrum ruber* sp. nov.

Materials and Methods

Strain isolation and culture conditions

Strain MBLA0099^T was isolated from seawater samples collected from the Yellow Sea near Yeongheung Island in the Republic of Korea (37° 15′ 22.36 N, 126° 30′ 03.35 E). The seawater samples were serially diluted with a 20% (w/v) sterile NaCl solution, and then spread onto ATCC 1176 medium (156 g/L of NaCl, 13 g/L of $MgCl_2{\cdot}6H_2O$, 20 g/L of $MgSO_4{\cdot}7H_2O$, 1 g/L of $CaCl_2$ $6H_2O$, 4 g/L of KCl, 0.2 g/L of $NaHCO_3$, 0.5 g/L of NaBr, 5 g/L of yeast extract, 1 g/L of glucose, and adjusted to pH 7.0, using 1 M Tris-base buffer solution), which contained 2 % (w/v) agar and was adjusted to pH 7.0 using 1 M Tris-base buffer solution (Burns *et al.*, 2010). After incubating at 37°C for 2 weeks, the red-pigmented colonies were sub-cultured at least three times on the fresh ATCC 1176 medium to obtain pure colonies. Finally, one strain designated as MBLA0099^T was routinely cultured on ATCC 1176 at 37°C and stored as a 25% (w/v) glycerol stock solution at -80°C.

Whole-genome sequencing, verification of authenticity, and contamination of the genome assembly

Genomic DNA was extracted from strain MBLA0099^T using HiYieldTM Genomic DNA Mini Kit (RBC Bioscience). The whole-genome sequence of the strain MBLA0099^T was obtained using a Pacific Biosciences RS II instrument with P6-C4 chemistry. *De novo* genome assembly was performed using Flye assembler 2.7 software with default parameters in the PacBio SMRT Analysis v. 2.3.0 (Chin *et al.*, 2013). The complete genome sequence of strain MBLA0099^T has been deposited in the National Center for Biotechnology Information (NCBI) GenBank database (accession number: CP-073695).

A partial 16S rRNA gene sequence was obtained using conventional Sanger sequencing. The 16S rRNA gene was amplified by polymerase chain reaction (PCR) using 18F (5′-ATTCCGGTTGATCCTGCC-3′) and 1518R (5′-AGGAGG TGATCCAGCCGC-3′) as an archaea-specific primer set (Cui *et al.*, 2009). The PCR products were purified using a QIA Quick PCR Purification Kit (Qiagen). The purified PCR products were sent to Macrogen Co., Ltd. for sequence analysis. Sequenced products were assembled using the SeqManTM II expert sequence analysis software.

The authenticity and absence of contamination of the genome of strain MBLA0099^T were verified per the proposed minimum standards for the use of genome data for the taxonomy of prokaryotes (Chun *et al.*, 2018). Authenticity was determined by comparing each 16S rRNA gene sequence obtained by conventional Sanger sequencing and extracted from the whole-genome sequencing results. Contamination in the genome assembly was verified using the ContEst16S algorithm to compare the genome-based 16S rRNA gene with the partial 16S rRNA gene (https://www.ezbiocloud.net/tools/contest16s) (Lee *et al.*, 2017).

Phylogenetic and genomic analysis

Phylogenetic analysis between strain MBLA0099^T and closely related species was performed using 16S rRNA gene sequences. The 16S rRNA gene sequence of strain MBLA0099^T was compared with those of other related species using EzBioCloud (https://www.ezbiocloud.net/identify). Multiple sequence alignments were performed using the ClustalW tool in BioEdit to compare the sequence similarity between strain MBLA0099^T and other species (Hall, 1999). Phylogenetic trees were constructed using the phylogeny build application in MEGA 7.0, based on the 16S rRNA gene sequences (Kumar *et al.*, 2016). Three algorithms, maximum likelihood (ML), neighbor-joining (NJ), and maximum parsimony (MP), were combined to calculate the sequence relatedness (Kluge and Farris, 1969; Felsenstein, 1981; Saitou and Nei, 1987). Phylogenetic trees were constructed using the bootstrap method and the values of bootstrap were 1,000 replicates. The Kimura two-parameter substitution model was selected to calculate the evolutionary distances of all species. *Halobacterium salinarum* DSM 3754^T was used as the outgroup taxon.

All the available genomes of the genus *Halorubrum*. were obtained from the NCBI genome database (http://www.ncbi.nlm.nih.gov/genome/). Ortho-average nucleotide identity (OrthoANI), average amino acid identity (AAI) and *in silico*

DNA-DNA hybridization (*is*DDH) were used to calculate genomic relatedness and delineate the microbial species. Ortho-ANI values among strain MBLA0099^T and other species of the genus *Halorubrum* were calculated using the OAT software version 0.93.1 to analyze genomic relatedness (Lee *et al.*, 2016). AAI values were calculated using the EzAAI tool (Kim *et al.*, 2021). *Is*DDH values were obtained from the Genome-to-Genome Distance Calculator (GGDC 2.1: http://ggdc.dsmz.de/distcalc2.php) using the recommended BLAST+ alignment and formula 2 (identities/HSPlength) (Meier-Kolthoff *et al.*, 2013).

Phenotypic characterization

All experiments were conducted using cultures grown at 37°C in ATCC 1176 solid and liquid media. Cell morphology was examined using light microscopy model CX 23 (Olympus) and LIBRA 120 transmission electron microscopy (Carl Zeiss). Gram staining was performed using a Gram stain kit (bioWORLD), according to the manufacturer's instructions. A cell motility test was performed on 0.5% semi-solid ATCC 1176 agar test tubes by stabbing inoculation and monitored colonies spreading or not for 7 days (Tittsler and Sandholzer, 1936). To assess the salinity concentration for growth, cells were cultivated in ATCC 1176 medium at intervals of 2.5%, ranging from 2.5% to 30% (w/v) NaCl concentrations. The Mg^{2+} requirement was tested by adding $MgCl_2{\cdot}6H_2O$ at intervals of 1%, ranging from 0% to 12%. The optimal growth pH of strain MBLA0099^T was assessed in increments of 0.5 units from pH 5.0 to 10.0 using the following buffers: 10 mM 2-(*N*-morpholino) ethane sulfonic acid (pH 5.0–6.0), 10 mM bis-Tris propane (pH 6.5–9.0), and 10 mM 3-(cyclohexylamino)-1-propane sulfonic acid (pH 9.5–10.0). Strain MBLA-0099^T was cultured and incubated at 4, 10, 20, 25, 30, 37, 40, 45, 50, and 55°C to determine the range of growth temperatures. Anaerobic growth was tested on ATCC 1176 medium supplemented with 5 g/L of L-arginine, trimethylamine *N*-oxide (TMAO), and dimethyl sulfoxide (DMSO) using a GasPak^{TM} EZ anaerobic gas generating pouch system with an indicator (BD Biosciences). Catalase and oxidase activities were tested using 3% (v/v) H_2O_2 and 1% tetramethyl-*p*-phenylenediamine solution and cell colonies were treated directly. Hydrolysis tests were performed by adding to ATCC 1176 medium with 0.2% (w/v) starch, 0.5% (w/v) casein, 1% (w/v) gelatin, and 1% (w/v) Tween 20, 40, and 80 (Benson, 2002). H_2S formation was tested by cultivation on ATCC 1176 broth containing 5 g/L of sodium thiosulfate using lead acetate paper. Indole formation, urease activity, and nitrate reduction were assessed using previously described methods (Holding and Collee, 1971; Smibert and Krieg, 1994). The following energy sources were added at 0.1% (w/v) to the media for the assimilation test: acetate, L-alanine, arabinose, L-arginine, citrate, fructose, fumarate, D-galactose, glucose, L-glutamate, glycerol, glycine, L-histidine, DL-lactate, lactose, L-lysine, L-malate, maltose, mannitol, D-mannose, L-ornithine, raffinose, rhamnose, ribose, starch, D-sorbitol, sucrose, succinate, trehalose, and xylose. Antibiotic susceptibility tests were performed on ATCC 1176 agar plates at 37°C for 7 days using the paper disc method (Bauer *et al.*, 1966). The antibiotics used in this study were ampicillin (10 µg), aphidicolin (50 µg), bacitracin (50 µg), chloramphenicol (50 µg), cephalothin (30 µg), erythromycin (25 µg), gentamicin (30 µg), kanamycin (30 µg), lincomycin (15 µg), neomycin (30 µg), norfloxacin (20 µg), novobiocin (10 µg), penicillin G (20 IU), rifampin (50 µg), streptomycin (50 µg), and tetracycline (30 µg).

Chemotaxonomic characterization

Polar lipids were extracted and separated using the method described previously (Minnikin *et al.*, 1984). To investigate polar lipid profiles, strain MBLA0099^T cells were freeze-dried, and the two-dimensional chromatographic method was performed using 10 × 10 cm silica gel 60 F254 (Merck) and detected using Molybdophosphoric acid, Zinzadze's reagent, and α-naphthol reagent.

Pan-genome analysis

Pan-genome analysis was performed using the Bacterial Pan-Genome Analysis (BPGA) software (Chaudhari *et al.*, 2016). Genomes of the members of the genus *Halorubrum* and strain MBLA0099^T were defined as core (conserved for all strains), accessory (shared by more than two species), and unique (strain-specific) pan-genome orthologous groups (POGs). Pan-genome function and pathway analyses were constructed based on the COG (https://www.ncbi.nlm.nih.gov/research/cog/) and Kyoto Encyclopedia of Genes and Genomes (KEGG) (https://www.genome.jp/kegg/) databases for representative sequences of all orthologous gene families (Kanehisa and Goto, 2000). A comparative functional analysis of the core, accessory, and unique POGs was performed. Unique genes classified from strain MBLA0099^T were annotated according to the KEGG database. To cluster COG and KEGG pan-genome POGs, the USEARCH algorithm was used with a 50% sequence identity cut-off value. All results of the plotting data in this analysis were visualized using Gnuplot 4.6.6. Multiple sequence alignment (MUSCLE) (Edgar, 2004).

Genome annotation

Gene prediction and comprehensive gene annotation were performed using the NCBI Prokaryotic Genome Annotation Pipeline (PGAP) (Zhao *et al.*, 2012). Clusters of Orthologous Groups (COG) of the predicted genes were categorized using eggNOG v5.0 for homology search (Huerta-Cepas *et al.*, 2017, 2019). The secondary metabolite biosynthetic gene clusters were identified using antiSMASH 6.0 software with strict detection criteria and additional features including KnownClusterBlast, ClusterBlast, SubClusterBlast, MIBiG comparison, ActiveSiteFinder, and RREFinder (https://antismash.secondarymetabolites.org/) (Blin *et al.*, 2019). Potential virulence genes were identified using a virulence factor database (VFDB) with the VFDB core dataset – of proteins associated with experimentally verified virulence factors (Chen *et al.*, 2005).

Carotenoid production and extraction

Seed culture of strain MBLA0099^T was cultivated in ATCC 1176 broth medium (20 ml in 50 ml conical tube) at 37°C, 200 rpm, for 2 days when $OD_{600\ nm}$ reaches approximately 1.0. After, submerged cultivation (80 ml medium in 200 ml

Erlenmeyer flasks) was carried out under the same conditions for 10 days with 1% (v/v) inoculation. In this experiment, multiple flasks more than 3 times were run at the same time in different media conditions for reproducibility.

Cell pellets were harvested, treated with acetone/methanol (7:3 v/v), and vortexed for more than 30 sec. The pellets were incubated at 37°C and 180 rpm for 2 h in dark conditions to decolorate sufficiently. Then, centrifuged at 4°C and 12,000 × *g* for 15 min to obtain the upper red organic-solvent layer. The upper organic layer of the extract was pooled and evaporated with a smart evaporator C1 (BioChromato Inc) at 50°C enough and re-dissolved in 100% methanol. The methanolic extract was subsequently filtered through a 0.2 μm pore size cellulose acetate membrane (GVS Korea Ltd.). The filtered carotenoid extract was conserved at -20°C in dark conditions. The carotenoid extract derived from strain MBLA0099^T was measured using a UV-1280 Shimadzu UV Visible spectrophotometer (Shimadzu) for primary confirmation. The maximum absorption spectra of the carotenoid extracts were obtained by spectrometry in the wavelength range of 300–600 nm. The spectra of the carotenoid extracts were displayed using the UV Probe spectrum program (Shimadzu).

Chromatographic analysis

Thin-layer chromatography (TLC) was performed on silica gel plates to quantify and confirm the presence of the extracts of strain MBLA0099^T. A solvent mixture of heptane/acetone (1:1, v/v) was used for the mobile phase and eluted for 30 min for separation via TLC analysis. Silica gel corresponding to the visualized band was scraped from the respective spots. The scraped silica gel was dissolved in 100% methanol and centrifuged at 4°C at 12,000 × *g* for 15 min.

Each methanolic extract obtained after centrifugation was filtered and analyzed by high-performance liquid chromatography (HPLC). The sorted carotenoid extracts were analyzed using a YL9100 HPLC system equipped with a YL9160 photodiode array (PDA) detector (Youngin Chromass). Chromatographic analysis was performed on a reverse-phase Syncronis C18 (Thermo Scientific) column (250 mm × 4.6 mm, 5 μm). The mobile phase was an isocratic eluent using 100% methanol, and the elution flow rate was 1.0 ml/min for 40 min. The eluent was detected at 490 nm, and online spectra were recorded between 300 and 600 nm. The chromatograms were monitored by measuring the maximum absorbance (λ_{max}) using a PDA detector.

The standard material 'Halorubin' was obtained from Halotek (https://halotek.de/) to identify the bacterioruberin production by the strain MBLA0099^T.

External stresses-induced carotenoid production

All culture experiments were performed in 200 ml Erlenmeyer with 80 ml culture media. To compare the carotenoid production level and cell growth in various stress conditions. In the case of pH stress, the pH was adjusted to 6.0, 7.0, 8.0, and 9.0, based on the employment of 10 mM 2-(N-morpholino) ethane sulfonic acid (pH 6.0) and 10 mM bis-Tris propane (pH 7.0–9.0) buffer. Additionally, the oxidative stress was evaluated with applying shaking conditions (0, 100, and 200 rpm). For the salinity stresses, both of sodium chloride (10–30%, w/v) and magnesium sulfate (0–5%, w/v) were initially applied to the culture medium to monitor the carotenoid production level.

Antibacterial activity of the carotenoid extract

The agar disk-diffusion method was used to determine the antibacterial susceptibility test (Balouiri *et al.*, 2016). The five pathogens (*B. cereus*, *E. coli*, *L. monocytogenes*, *S. aeruginosa*, and *S. aureus*) were cultivated in nutrient broth. For standardized inoculum of the test pathogens, each culture broths were diluted to an $OD_{600\ nm}$ of 1.0 and were inoculated by spreading 100 μl of diluted broth culture on nutrient agar plates. Then, 6 mm filter paper discs were placed on the agar surface and various concentration of carotenoid extract (2.5–100 μg/ml) dissolved in DMSO were loaded on discs, respectively. Cultured plates were incubated at 30 or 37°C for 48 h. A commercial antibacterial compound streptomycin (10 μg/ml) was used as positive, while DMSO was used as negative control in this test.

Antioxidant potential of the carotenoid extract

Antioxidant activity was evaluated by free-radical scavenging activity of extracted carotenoids with 0.2 mM DPPH (1,1-Diphenyl-2-picryl-hydrazine) solution (Alvares and Furtado, 2021). Methanolic carotenoid extract (10 μg/ml) was mixed with 1 ml of 0.2 mM methanolic DPPH (1:2, v/v) and incubated at room temperature for 30 min. Thereafter, the absorbances were monitored by using UV/VIS spectrophotometer at 517 nm. Percent of the DPPH scavenging effect was calculated by the following equation: % DPPH scavenging effect = $[(A_0 - A_1) / A_0] \times 100$, where A_0 = absorbance of the control and A_1 = absorbance of the sample.

Table 1. General characterizations of the genome of strain MBLA0099^T

Attribute	Characteristics
Sequencing platforms	PacBio
Assembler	FLYE v. 2.7
Genome coverage	292.0x
Assembly status	Complete
Assembly size (bp)	3,021,820
G + C content of DNA (mol%)	68,9
N50	3,021,820
Total contigs	1
Circular DNA	1
Accession number	CP073695
Total genes	2,975
Total CDS	2,919
Coding genes	2,786
Pseudo genes	133
Number of RNAs	56
- rRNA genes (5S, 16S, 23S)	2, 2, 2
- tRNAs	48
- ncRNAs	2

Results and Discussion

Genomic features, verification of authenticity, and contamination of the genome assembly

The genome sequence of strain MBLA0099^T comprised one complete chromosome (3,021,820 bp), and the G + C content of DNA was 68.9 mol%. Strain MBLA0099^T was predicted to harbor 2,975 genes including 2,786 coding genes, 56 RNA genes, and 133 pseudogenes. The number of rRNAs, tRNAs, and ncRNAs were 6, 48, and 2. More detailed general genomic features of the strain MBLA0099^T are presented in Table 1.

The comparison of 16S rRNA gene sequences obtained from whole-genome sequencing and conventional Sanger sequencing confirmed 100% similarity for strain MBLA0099^T. The authenticity and contamination of the genome of strain MBLA0099^T were verified as the genome sequences were not contaminated.

Phylogenetic analysis

Two 16S rRNA gene sequences of strain MBLA0099^T (1,477 and 1,476 bp, respectively) were obtained by whole-genome sequencing as mentioned above. In phylogenetic analysis, strain MBLA0099^T and other closely related species showed 99.1% 16S rRNA gene sequence similarity (Supplementary data Table S1). The closest phylogenetic relatives and similarities were identified as *Hrr. sodomense* DSM 3755^T (99.1%), *Hrr. trapanicum* NRC 34021^T (99.0%), and *Hrr. coriense* Ch^T (98.6%). Furthermore, the phylogenetic tree based on 16S rRNA gene sequences showed that the closest clustered species to strain MBLA0099^T was *Hrr. distributum* JCM 9100^T (73, 70, and 66 in ML, NJ, and MP trees, respectively). Strain MBLA0099^T and *Hrr. distributum* JCM 9100^T clustered with *Hrr. coriense* Ch^T (Fig. 1). According to the phylogenetic analysis based on 16S rRNA gene sequences, strain MBLA0099^T was predicted to belong to the genus *Halorubrum*.

Genome analysis

The OrthoANI values computed by comparison between strain MBLA0099^T and other species of the genus *Halorubrum* ranged from 77.4 to 91.9%. The AAI showed between strain MBLA0099^T and other species with values ranging from 72.8 to 92.8%. The *is*DDH values obtained by comparison between strain MBLA0099^T and other species of the genus *Halorubrum* did not exceed 44.2% (Table 2). According to the suggested cut-off values of OrthoANI, AAI, and *is*DDH for species delineation (less than 95–96%. 95–96%, and 70%, respectively) (Konstantinidis and Tiedje, 2005; Meier-Kolthoff *et al*., 2013; Lee *et al*., 2016), the calculated values based on the comparative genome analysis results indicate that strain MBLA0099^T is distinguished from other previously reported *Halorubrum* species. The use of whole-genome sequences for the taxonomy of prokaryotes, despite showing 98.7% or higher 16S rRNA gene similarity, a combination of 16S rRNA gene sequence similarity, and the overall genome data index, can be used in a systematic process to identify and recognize a new species (Chun *et al*., 2018).

Morphological, physiological, and biochemical characterization

Cells of the novel strain MBLA0099^T were Gram-negative, non-motile, and rod-shaped, having a width of 1.0–1.7 μm and a length of 5.8–6.0 μm as revealed by TEM (Supplementary data Fig. S1). Colonies were red and sticky on ATCC 1176 incubated at 37°C for 7 days. Growth of strain MBLA0099^T occurred at 10–45°C (optimum, 37°C), pH 5.5–9.0 (optimum, pH 7.0), and 7.5–30% (w/v) NaCl (optimum,

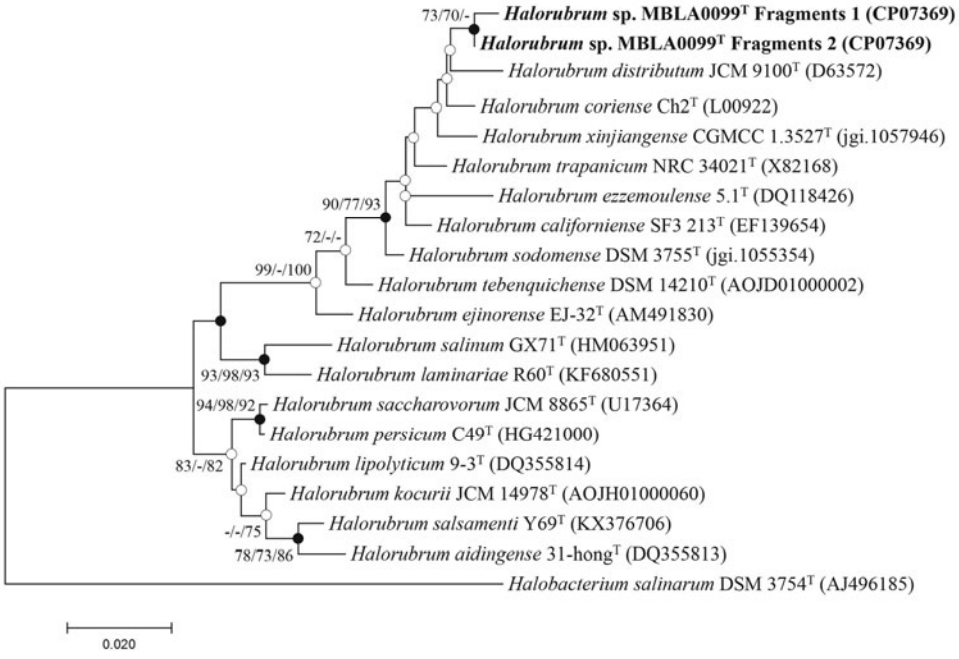

Fig. 1. Maximum likelihood (ML) phylogenetic tree of strain MBLA0099^T based on the 16S rRNA gene sequences. Phylogenetic tree was constructed with closely-related speceis of the genus *Halorubrum*. The closed circles represent nodes recovered by both the neighbor-joining (NJ) and maximum parsimony (MP) algorithms; the open circles represent nodes recovered by either NJ or MP. The numbers on the nodes indicate the bootstrap values (> 70%) calculated using the ML/NJ/MP probabilities. Bar, 0.02 accumulated changes per nucleotide, respectively.

Table 2. **Overall DNA relatedness based on the genome data between strain MBLA0099^T and other species of the genus *Halorubrum***

Taxon	ANI (%)	*is*DDH (%)	AAI (%)	Size (Mb)	G + C content (mol%)	Accession no.
Hrr. litoreum JCM 13561^T	91.9	44.2	92.8	3.14	68.9	AOJF00000000
Hrr. terrestre JCM 10247^T	91.9	44.2	92.5	3.38	68.0	AOIW00000000
Hrr. distributum JCM 10118^T	91.9	44.1	92.6	3.31	68.1	AOJN00000000
Hrr. arcis JCM 13916^T	91.8	43.7	92.6	3.38	67.3	AOJJ00000000
Hrr. salinarum RHB-C^T	89.5	36.6	89.8	3.34	68.7	CP053941
Hrr. xinjiangense CGMCC 1.3527^T	89.4	36.6	90.1	3.26	68.3	FNBO00000000
Hrr. californiensis DSM 19288^T	89.3	36.3	89.8	3.68	66.2	AOJK00000000
Hrr. sodomense DSM 3755^T	89.1	35.5	89.1	3.03	69.0	FOYN00000000
Hrr. trapanicum DSM 12287^T	88.8	35.0	89.2	3.08	68.0	JAGGKE000000000
Hrr. ezzemoulense DSM 17463^T	88.1	33.4	88.0	3.59	66.8	ATXS00000000
Hrr. chaoviator DSM 19316^T	87.9	33.5	88.0	3.66	66.5	NDWV00000000
Hrr. coriense DSM 10284^T	87.8	33.0	87.5	3.65	67.0	AOJL00000000
Hrr. tebenquichense DSM 14210^T	87.5	31.7	87.3	3.33	68.0	AOJD00000000
Hrr. lipolyticum 9-3^T	84.0	26.8	81.1	3.42	68.0	AOJG00000000
Hrr. amylolyticum ZC67^T	83.9	26.9	81.2	3.63	66.3	SDJP00000000
Hrr. saccharovorum JCM 8865^T	83.9	26.6	80.9	3.35	66.7	AOJE00000000
Hrr. halophilum b8^T	83.8	26.8	81.4	3.47	65.5	BBJP00000000
Hrr. salsamenti Y69^T	83.8	26.5	81.0	3.67	66.0	VCNL00000000
Hrr. depositum Y78^T	83.8	26.5	81.2	3.18	68.6	VCNM00000000
Hrr. persicum C49^T	83.5	26.5	81.0	3.58	66.9	NHOA00000000
Hrr. kocurii JCM 14978^T	83.3	26.6	80.8	3.62	66.9	AOJH00000000
Hrr. lacusprofundi ATCC 49239^T	83.1	25.7	81.1	3.69	64.0	CP001365-7
Hrr. aidingense 1-hong^T	82.6	25.5	80.0	3.11	67.2	AOJI00000000
Hrr. aethiopicum SAH-A6^T	82.1	25.0	77.3	3.33	68.0	LOAJ00000000
Hrr. halodurans Cb34^T	81.6	24.9	76.9	3.32	67.7	NHPJ00000000
Hrr. aquaticum CGMCC 1.6377^T	81.4	24.5	76.8	3.18	67.4	FOPZ00000000
Hrr. cibi DSM 19504^T	81.2	24.4	76.9	3.18	66.8	FXTD00000000
Hrr. alkaliphilum DSM 23564^T	79.9	23.3	76.7	3.10	64.5	JAGGKQ000000000
Hrr. vacuolatum DSM 8800^T	78.0	22.6	72.8	3.48	62.9	FZNQ00000000

17.5%). The test of the Mg^{2+} requirement showed that strain MBLA0099^T could grow without Mg^{2+} under culture conditions. Strain MBLA0099^T did not hydrolyze casein, gelatin, starch, or Tweens 20, 40, or 80. Positive reactions were detected in the catalase and oxidase tests. Strain MBLA0099^T was negative for indole formation, H_2S formation, dissimilatory nitrate and nitrite reduction, and urease activity. Under anaerobic conditions, strain MBLA0099^T did not use DMSO,

Table 3. **Distinguishing characteristics of strain MBLA0099^T and other species of the genus *Halorubrum* (*Hrr.*)**
Taxa: 1, Strain MBLA0099^T; 2, *Hrr. californiense* SF3-213^T; 3, *Hrr. coriense* Ch^T; 4, *Hrr. distributum* JCM 9100^T; 5, *Hrr. ezzemoulense* CECT 7099^T; 6, *Hrr. sodomense* DSM 3755^T; 7, *Hrr. trapanicum* NRC 34021^T; 8, *Hrr. xinjiangense* AS 1.3527^T). +, Positive; -, negative.

Characteristics	1	2	3	4	5	6	7	8
Motility	-	+	+	+	+	+	-	+
Temperature range (°C) (optimum)	10–45 (37)	20–45 (37)	15–40 (37)	15–40 (37)	20–45 (37)	10–45 (37)	10–45 (37)	10–45 (37)
NaCl range (M) (optimum)	1.3–5.1 (3.0)	2.5–5.0 (3.4)	2.0–5.2 (3.4)	1.7–5.2 (3.4)	2.5–4.3 (3.4)	0.5–4.3 (2.6)	2.5–5.2 (3.4)	2.0–5.2 (3.4)
pH range (optimum)	5.5–9.0 (7.0)	6.5–8.5 (7.0)	6.0–9.0 (7.0)	6.0–9.0 (7.5)	6.5–9.0 (7.5)	6.0–9.0 (7.0)	6.0–8.0 (7.0)	6.0–10.0 (7.0)
Nitrate reduction	-	+	-	+	-	-	+	-
Indole production	-	+	-	-	-	-	-	-
Casein hydrolysis	-	+	-	-	-	-	-	-
Mg^{2+} requirement	-	+	+	-	-	+	-	-
Utilization of								
D-Glucose	+	+	+	-	-	+	+	+
D-Galactose	+	+	+	-	-	+	+	-
Lactose	+	+	+	-	-	+	-	-
D-Fructose	+	-	-	-	+	+	+	+
Mannose	+	-	+	+	-	-	+	-
PGS present	+	+[a]	+[b]	+[b]	+[c]	+[d]	+[d]	+[e]

[a] Pesenti *et al.* (2008); [b] Ventosa *et al.* (2004); [c] Kharroub *et al.* (2006); [d] McGenity and Grant (1995); [e] Feng *et al.* (2004).

TMAO, L-arginine, or nitrate as electron acceptors. The following substrates were used as energy sources: glycerol, D-galactose, D-glucose, D-fructose, D-mannitol, D-maltose, sucrose, D-raffinose, D-mannose, and D-lactose. Strain MBLA0099^T was susceptible to ampicillin, gentamycin, kanamycin, lincomycin, neomycin, norfloxacin, and streptomycin, whereas it was resistant to aphidicolin, bacitracin, chloramphenicol, cephalothin, erythromycin, novobiocin, penicillin G, rifampin, and tetracycline. This antibiotic testing of the strain MBLA0099^T indicated the difference with the previously reported *Halorubrum* species with focusing on ampicillin and streptomycin (resistant), and bacitracin (sensitive) for *Hrr. californiense* SF3-213^T (Pesenti *et al.*, 2008), *Hrr. distributum* JCM 9100^T (Ventosa *et al.*, 2004), and *Hrr. ezzenmoulense* CECT 7099^T (Kharroub *et al.*, 2006). Other characteristics of strain MBLA0099^T and related species are shown in Table 3.

Chemotaxonomic analysis

A two-dimensional thin-layer chromatogram showed that the major polar lipids in strain MBLA0099^T were PG, PGP-Me, PGS, and S-DGD-3 (Supplementary data Fig. S2). In addition, minor lipids such as two unidentified glycolipids, two unidentified phospholipids, and eight unidentified lipids were detected. The major polar lipid profile of strain MBLA0099^T was similar to that of the members of the genus *Halorubrum*. Based on the chemotaxonomic analysis, strain MBLA0099^T was proposed as a species belonging to the genus *Halorubrum*.

Pan-genome analysis

Pan-genome analysis shows that strain MBLA0099^T and 29 species of the genus *Halorubrum* had a total of 13,976 POGs, 1,072 core POGs, 6,063 accessory POGs, and 6,841 unique POGs. Within genomes, the core and accessory genes of all *Halorubrum* species constitute 31.7–39.6% and 38.1–63.1% of protein-coding genes, respectively (Table 4). In addition, strain MBLA0099^T had 84 (3.1%) unique POGs, and other species had a variety of unique strain-specific POGs. This observation suggests that all species analyzed by the pan-genome analysis were distinct. According to the COG database, the number of unique POGs of strain MBLA0099^T was 30, of which 21 were predicted as functional annotations, and most were categorized as functions related to cell wall/membrane/envelope biogenesis (M, 6, 20%) and inorganic ion transport and metabolism (P, 6, 20%). In the other six categories, POGs not found in any other species of the genus *Halorubrum* were also detected in the strain MBLA0099^T. According to the KEGG database, 20 POGs were confirmed as KEGG categorizations of unique genes, of which only seven POGs were defined as functional KEGG annotations (Supplementary data Table S2). Among these, metabolism is predominant. In particular, the function of the K03186 gene, described as *ubiX*, *bsdB*, *PAD1*, and flavin prenyltransferase, is related to terpenoid-quinone and terpenoid backbone biosynthesis. However, it was difficult to confirm that the unique genes of strain MBLA0099^T were related to novel biosynthetic or metabolic pathways generally not found in the genus *Halorubrum*. In addition, the number of exclusively absent genes appeared to be exceptionally high in strain MBLA0099^T compared to that in other *Halorubrum* species (Supplementary data Table S3). The exclusive presence and absence of genes indicate that strain MBLA0099^T is different from other previously characterized species of the genus *Halorubrum*.

Functional gene annotations

COG analysis shows that a total of 2,843 genes were present in strain MBLA0099^T, and 1,703 (59.9%) genes associated with the 19 general COG functional categories were classified as functional genes, excluding those classified as functionally unknown (S). The most abundant predicted genes in strain MBLA0099^T belonged to the COG categories of amino acid transport and metabolism (E, 229, 8.1%), inorganic ion transport and metabolism (P, 175, 6.2%), translation, ribosomal structure, and biogenesis (J, 152, 5.3%), energy production and conversion (C, 146, 5.1%), and replication, recombination, and repair (L, 136, 4.8%) (Supplementary data Table S4). A recent study of comprehensive haloarchaeal conserved proteins found that approximately 33% of core clusters were predicted to function in metabolism including amino acid transport and metabolism, with the most frequent portion (Capes *et al.*, 2012). Haloarchaea generally prefers amino acid

Table 4. The fraction of core, accessory, and unique genes of strain MBLA-0099^T and other species of the genus *Halorubrum* (*Hrr.*) used for pan-genomic analysis

Organism	Genes	Core (%)	Accessory (%)	Unique (%)
Strain MBLA0099^T	2,708	39.6	57.3	3.1
Hrr. litoreum JCM 13561^T	2,928	36.6	61.1	2.3
Hrr. terrestre JCM 10247^T	3,089	34.7	63.1	2.2
Hrr. distributum JCM 10118^T	3,007	35.7	61.6	2.7
Hrr. arcis JCM 13916^T	3,105	34.5	62.1	3.4
Hrr. xinjiangense CGMCC 1.3527^T	3,026	35.4	59.7	4.8
Hrr. californiensis DSM 19288^T	3,227	33.2	59.2	7.6
Hrr. sodomense DSM 3755^T	2,926	36.6	59.1	4.2
Hrr. trapanicum DSM 12287^T	2,907	36.9	57.9	5.2
Hrr. chaoviator DSM 19316^T	3,386	31.7	61.7	6.6
Hrr. ezzemoulense DSM 17463^T	3,144	34.1	61.2	4.7
Hrr. coriense DSM 10284^T	3,273	32,8	59,4	7.8
Hrr. tebenquichense DSM 14210^T	3,086	34.7	58.5	6.8
Hrr. amylolyticum ZC67^T	3,162	33.9	57.9	8.2
Hrr. halophilum b8^T	3,286	32.6	59.3	8.1
Hrr. lipolyticum 9-3^T	3,118	34.4	59.1	6.5
Hrr. saccharovorum JCM 8865^T	3,107	34.5	57.4	8.1
Hrr. kocurii JCM 14978^T	3,253	33.0	60.3	6.8
Hrr. persicum C49^T	3,072	34.9	57.3	7.8
Hrr. salsamenti Y69^T	3,280	32.7	60.5	6.8
Hrr. depositum Y78^T	3,019	35.5	54.2	10.3
Hrr. lacusprofundi ATCC 49239^T	3,300	32.5	54.2	13.3
Hrr. aidingense 1-hong^T	2,899	37.0	55.7	7.3
Hrr. aethiopicum SAH-A6^T	3,045	35.2	56.9	7.8
Hrr. halodurans Cb34^T	2,991	35.8	54.4	9.8
Hrr. aquaticum CGMCC 1.6377^T	3,006	35.7	59.1	5.2
Hrr. cibi DSM 19504^T	2,996	35.8	59.8	4.4
Hrr. vacuolatum DSM 8800^T	3,201	33.5	38.1	28.4
Hrr. salinarum RHB-C^T	3,137	34.2	59.7	6.1
Hrr. alkaliphilum DSM 23564^T	2,946	36.4	50.3	13.3

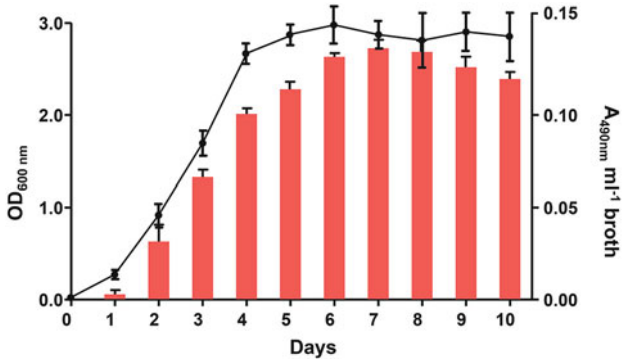

Fig. 2. Time-course profiles of cell growth and bacterioruberin production. Closed circles and red columns represented cell growth and bacterioruberin productivity by strain MBLA0099^T on ATCC 1176 medium for 10 days. Bars represent mean ± SD of three independent experiments.

utilization over carbon source utilization (Thombre *et al.*, 2016). In addition, the compatible solutes or osmolytes accumulated in haloarchaea are usually amino acids, and amino acid uptake is carried out by a Na^+ ion with an amino acid symporter at an extremely high salt concentration in the intracellular space (DasSarma and DasSarma, 2017). These gene distributions are predicted to be general characteristics of haloarchaea. No virulence factor was detected by VFDB in the genome of strain MBLA0099^T. This result indicates that the strain used in this study can be used in commercial applications including functional food and feed production.

Biosynthetic gene clusters (BGCs) predicted by antiSMASH show that the genome of strain MBLA0099^T had two BGCs responsible for the secondary metabolites of terpene. The terpene BGC related to carotenoid production revealed that the phytoene synthase gene (*crtB*) was annotated as a core gene. The BGCs investigated in strain MBLA0099^T shared no similarity with known pathways, according to KnownClusterBlast. However, ClusterBlast shows that two BGCs were the most similar gene clusters to *Hrr. sodomense* DSM 3755^T and *Hrr. xinjiangense* CGMCC 1.3527^T based on the reported type-strain (Supplementary data Table S5). One BGC located from nucleotide 568,265 to 588,625 in the genome was associated with carotenoid production, which is a type of terpene, and the other BGC located from nucleotide 2,074,027 to 2,095,088 in the genome was also related to carotenoid production. The terpene BGC genes detected in haloarchaea, such as *Halobacterium*, *Natrinema*, *Haloarcula*, *Haloferax*, and *Haloterrigena*, were associated with bacterioruberin production (Serrano *et al.*, 2021).

Carotenoid production

The growth curve and production of carotenoid on ATCC 1176 media were shown in Fig. 2. The absorbance at 490 nm ($A_{490\ nm}$ ml^{-1} broth) increased rapidly and peaked after 6 days of cultivation. There was no significant difference from 6 to 9 days of bacterioruberin production. The maximum carotenoid production of strain MBLA0099^T was 0.132 ± 0.001 $A_{490\ nm}$ ml^{-1} broth. Although strain MBLA0099^T is not superior productivity compared to other previous studies using *Haloferax mediterranei* (0.314 $A_{494\ nm}$ ml^{-1} or 3.3 μg/ml), it can be applied to increase the carotenoid productivity using stress conditions (starvation, salinity control, radiation, and light induction) and culture optimization (Fang *et al.*, 2010; Montero-Lobato *et al.*, 2018).

The carotenoid solution extracted from strain MBLA0099^T showed three photometric fingerprints, which are generally known as the characteristic absorptions of carotenoids. Bacterioruberin and its precursors exhibit characteristic spectral peaks of red carotenoids at nearly identical maximum absorption spectra for major three-fingered peaks and two

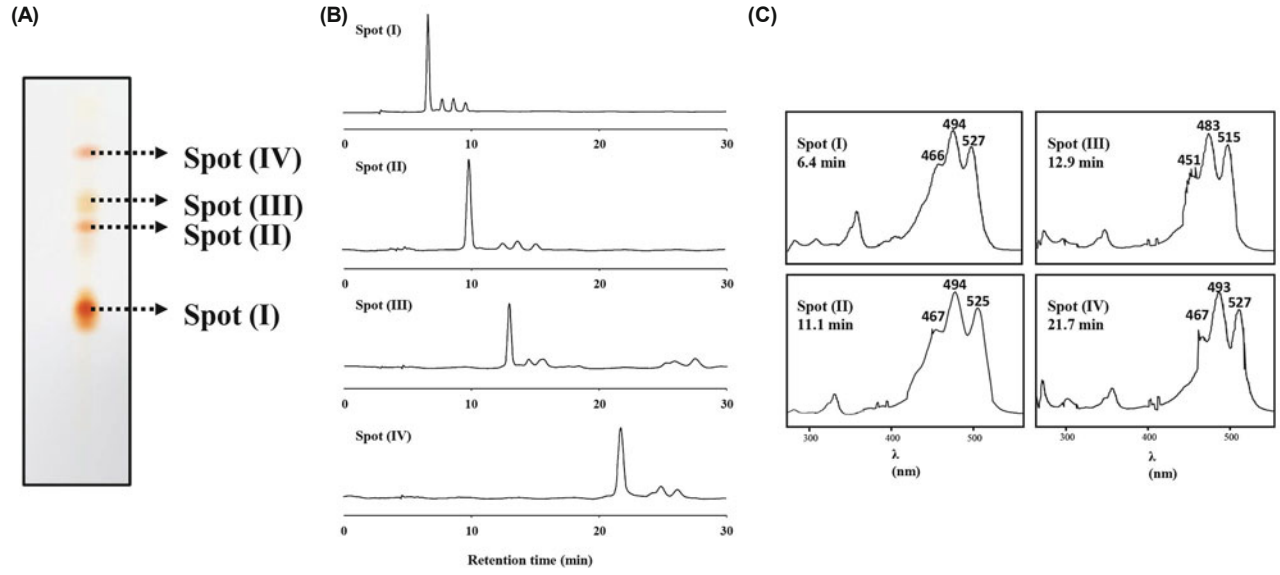

Fig. 3. Chromatographic and spectrometric analyses of sorted carotenoids extracted from strain MBLA0099^T. (A) Thin-layer chromatography profile of sorted carotenoids extracted from strain MBLA0099^T. (B) HPLC chromatogram for each sorted spot obtained by TLC, respectively. (C) UV visible absorption spectrum according to their chromatographic peaks using HPLC-PDA detector.

minor *cis* peaks, as previously reported (Britton, 1995). Carotenoid extract derived from strain MBLA0099^T showed maximum absorption peaks nearly at 464, 490, 523 nm, and two absorption peaks of approximately 370 and 385 nm (predicted *cis* peaks) were also detected by UV visible spectrometry (Supplementary data Fig. S3).

The separation and identification of carotenoids in the first extract were carried out by TLC analysis. As shown in Fig. 3, TLC revealed four major spots. After development, four spots were visualized, three of which were red (spots I, II, and IV) and the third orange (spot III) (Fig. 3A). The elution profile of the carotenoid extract of strain MBLA0099^T was predicted to contain bacterioruberin and its precursors (Fang *et al*., 2014). To isolate the main carotenoid compounds, the silica gel corresponding to the spot was treated with methanol, and the individual spots were analyzed by RP-HPLC at 490 nm and detected by PDA (Fig. 3B). Chromatograms of individual spots and the corresponding full-wavelength spectra were detected (Fig. 3C). Spot I had a visible spectral maximum of 494 nm with obvious absorption at approximately 466 and 527 nm, which is consistent with the absorption spectrum of bacterioruberin. Spot I contained predominant peaks eluting at 6.4 min. Spot II contained a predominant peak eluting at 11.1 min, of which the chromatographic components had a maximum absorption spectrum of 494 nm, including 467 and 525 nm. The chromatographic peak eluting at 12.9 min represents spot III; this component had a maximum absorption spectrum at 483 nm, including 451 and 515 nm. The absorption spectrum of spot III was different from that of the other three spots because of the number of carbons in the carotenoid backbone. Finally, spot IV contained a predominant peak eluting at 21.7 min in which the chromatographic component had a maximum absorption spectrum of 494 nm. The chromatographic profile of each spot revealed the presence of multiple molecules in the same band. These results led to the hypothesis that these bands contain a specific molecule present in several isomeric forms that migrated as a unique spot. The major carotenoid products of strain MBLA0099^T were predicted to be C_{50} bacterioruberin (spot I), C_{50} monoanhydrobacterioruberin (MABR) (spot II), C_{45} isopentenyldehydrorhodopsin (IDR) (spot III), and C_{50} bisanhydrobacterioruberin (BABR) (spot IV), based on a comparison of the observed spectral properties with those previously reported for haloarchaea carotenoids (Supplementary data Table S6) (Yatsunami *et al*., 2014). In addition, the comparison of standard material 'Halorubin' and the carotenoid extract from the strain MBLA0099^T revealed that the extract was identical to 'Halorubin' containing bacterioruberin and its intermediates (Supplementary data Fig. S4).

Bacterioruberin biosynthesis pathway of strain MBLA0099^T

According to genome annotation in this study (Supplementary data Table S7), strain MBLA0099^T uses the mevalonic acid (MVA) pathway for terpenoid backbone biosynthesis. The product of glycolysis synthesizes isopentenyl pyrophosphate (IPP) and dimethylallyl pyrophosphate (DMAPP) from acetyl-CoA through a series of enzyme reactions. Then, geranylgeranyl diphosphate synthase type I (*idsA*) participates in the terpenoid backbone biosynthesis of geranyl pyrophosphate (GPP), farnesyl pyrophosphate (FPP), and geranylgeranyl pyrophosphate (GGPP). Carotenoid biosynthesis begins with GGPP as a first precursor. C_{50} carotenoid bacterioruberin is probably synthesized subsequently by phytoene synthase (*crtB*), lycopene elongase (*lyeJ*), and carotenoid biosynthesis protein (*cruF*). Especially, *crtD* annotated with carotenoid 3,4-desaturase and phytoene desaturase (*crtI*) is predicted to be closely related to bacterioruberin biosynthesis as a bifunctional gene. The gene *crtI* which converts phytoene

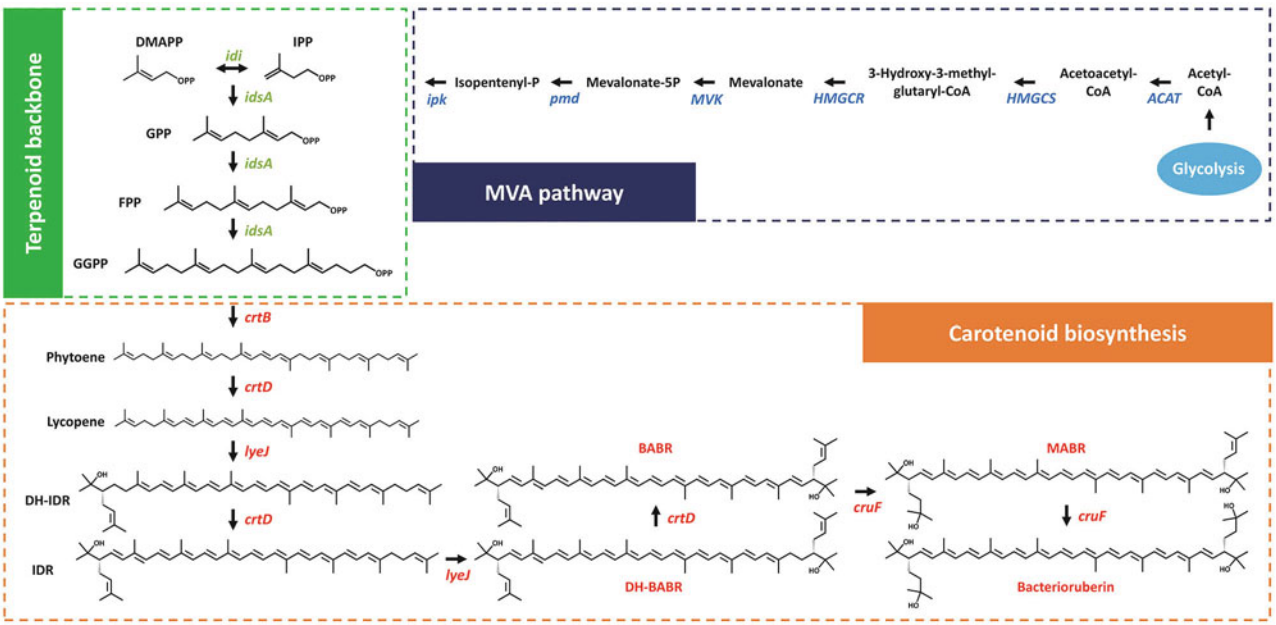

Fig. 4. **Predicted whole C_{50} carotenoid bacterioruberin biosynthesis pathway in strain MBLA0099^T based on the genome annotation.**

Table 5. Comparison of nucleotide and amino acid identities with amino acid (AA) counts in carotenoid biosynthetic genes between strain MBLA0099^T and other species known to produce bacterioruberin

Taxon	Genes from MBLA0099^T (AA)			
	crtB (321)	*crtD* (500)	*lyeJ* (311)	*cruF* (313)
Halorubrum ezzemoulense Fb21	93.1/94.7 (321)	92.4/95.6 (500)	89.5/83,9 (315)	87.5/89.1 (312)
Haloarcula japonica DSM 6131^T	65.0/56.2 (323)	72.3/71.0 (495)	59.2/59.3 (294)	57.0/61.6 (293)
Haloferax vocanii DS2^T	64.6/65.7 (339)	79.6/78.1 (500)	66.8/66.8 (301)	62.8/66.6 (293)
Halobacterium salinarum DSM 3754^T	60.1/54.0 (322)	73.0/70.0 (512)	61.5/63.5 (275)	58.2/63.1 (279)

to lycopene found within common organisms that produces C_{40} and C_{50} carotenoids, has not been identified in *Haloarcula japonica*, which had been however reported to biosynthesize the bacterioruberin as C_{50} carotenoid by the presence of *crtD* instead (Yang *et al.*, 2015). This previously reported results could support that two types of desaturation reactions in the bacterioruberin biosynthesis pathway maybe resulted from a single desaturase gene annotated *crtI* or *crtD* in haloarchaea, Accordingly, the absence of *crtI* in the genome of isolated strain MBLA0099^T suggests that *crtD* can perform the function of *crtI* instead in bacterioruberin biosynthesis. C_{40} phytoene is synthesized by *crtB* via two GGPP molecules and C_{40} lycopene is synthesized by *crtD*. Then, lycopene is used for C_{50} backbone biosynthesis with two IPP molecules using *lyeJ*. Immature C_{50} carotenoids such as DH-BABR, BABR, and MABR, are subsequently transformed to bacterioruberin by *crtD* and *cruF*, generating two double bonds and four hydroxyl groups. The predicted total C_{50} carotenoid bacterioruberin biosynthesis pathway of strain MBLA0099^T is shown in Fig. 4.

Three out of four genes related to carotenoid biosynthesis pathway are clustered well in the genome of strain MBLA-0099^T. A cluster of *crtD-lyeJ-cruF* is present from 1,312,293 to 1,315,677 bp of the genome of MBLA0099^T. This cluster is well conserved in four other species (*Halorubrum ezzemoulense* Fb21, *Haloarcula japonica* DSM 6131^T, *Halobacterium salinarum* DSM 3764^T, *Haloferax vocanii* DS2^T) known to produce bacterioruberin (Giani *et al.*, 2020). Compared to strain MBLA0099^T, four species show over 50% of nucleotide and amino acid identities harboring bacterioruberin biosynthetic genes (Table 5). *Halorubrum ezzemoulense* Fb21, which is classified as the same species of the genus was shown a high level of nucleotide and amino acid sequence identities (87.5–93.1% and 83.9–95.6%, respectively). These results suggest that bacterioruberin production-associated genes are conserved at a significantly high in the species of the same genus. Especially, the *crtD* gene, compared to other species of the different genera, is shown to be more conserved than other genes, with more than 70% of nucleotide and amino acid sequence identities. From this, it is predicted that the *crtD* gene is the most important gene within the bacterioruberin biosynthetic cluster. Whether *crtB* is located in the adjacent gene cluster or not is appeared differently for each species (Fig. 5). Phytoene is a precursor of β-carotene and/or retinal production in haloarchaea. The gene distribution results suggest that *crtB* is not involved only in the bacterior-

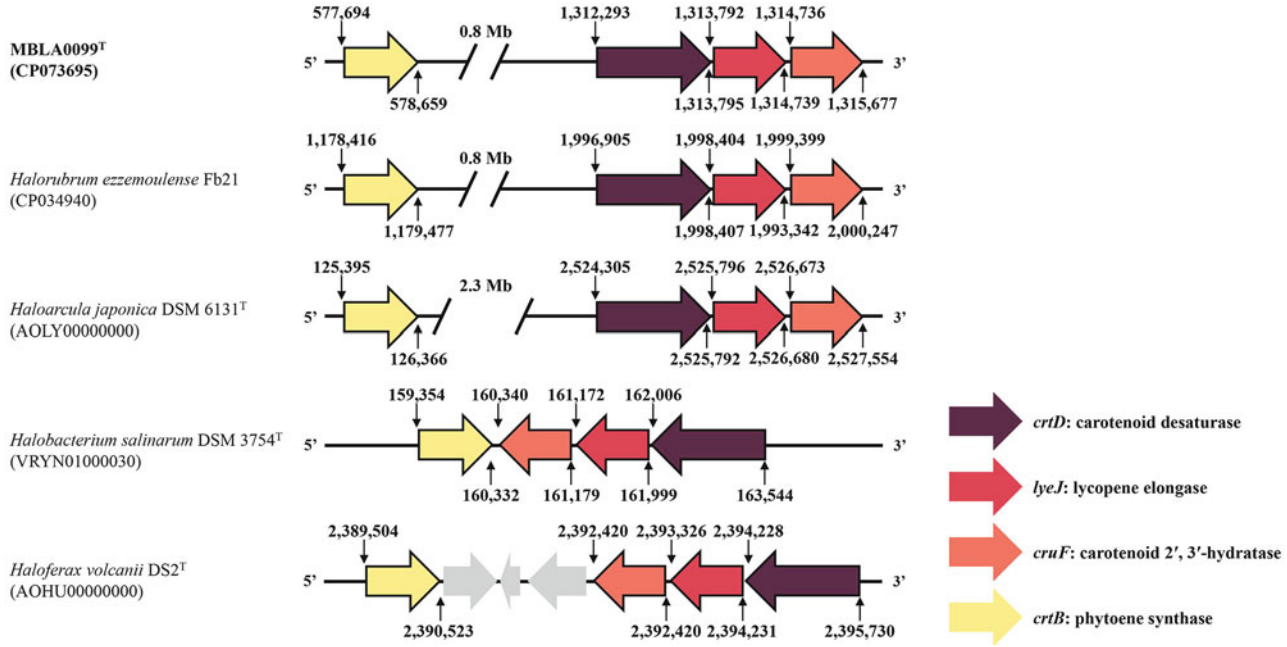

Fig. 5. Comparisons of genetic localization of bacterioruberin biosynthetic gene between strain MBLA0099^T and several haloarchaea species. Numbers indicate the start and end position of the genome and arrows indicate the direction of the genes.

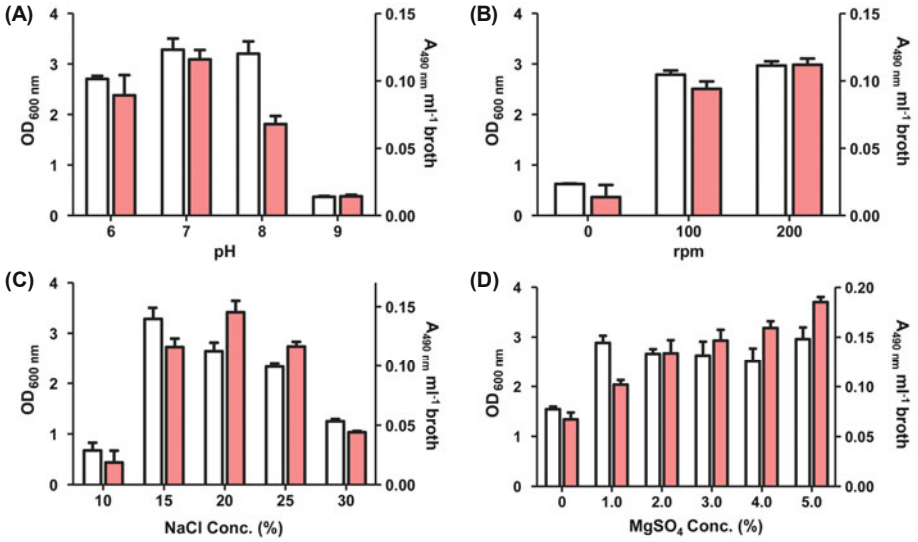

Fig. 6. Effects of external stresses including pH (A), shaking speed (B), sodium chloride (C), and magnesium sulfate (D) on cell growth (white bars) and C_{50} carotenoid production (pink bars) of the strain MBLA0099^T. All results from three independent experiments are represented as means ± standard deviation.

uberin biosynthesis. In addition, the difference in the clustering of bacterioruberin biosynthetic gene in haloarchaea may be occurred by evolutionary distance.

Effects of various stresses on C_{50} carotenoid production by the strain MBLA0099^T

Stressful environments often lead to the accumulation of carotenoids as a means of cellular defense (Paliwal *et al*., 2017). To evaluate the effects of various stresses on C_{50} carotenoid production and cell growth levels, the strain MBLA0099^T was cultivated at 37°C for 6 days. After the pH stress with the range from pH 6.0 to 9.0, the cell growth was similar to nearly neutral pH conditions, whereas the carotenoid production was obtained at 0.112 ± 0.005 A_{490nm} ml^{-1} at the pH 7.0 condition over which pH condition triggered the significant decrease of carotenoid production (Fig. 6A). This result could be resulted from the relation between the phenotypic characteristics of strain MBLA0099^T and the carotenoid production, since the members of the genus *Halorubrum* generally require neutral pH for the optimal growth (McGenity and Grant, 1995). To investigate the effect of oxidative stress, we applied the different shaking speeds from 0 to 200 rpm in the flask culture level, resulting that the maximum carotenoid production attained 0.116 ± 0.007 A_{490nm} ml^{-1} at 200 rpm, which were 8.2 and 1.2 times higher than 0 and 100 rpm (Fig. 6B). As the increase of shaking speed, the cell growth was also increased which was probably due to the characteristic of haloarchaea as aerobic microbes in general. In addition, it could be noted that the oxidative stress of haloarchaea cells according to the increase of shaking speed accelerated the carotenoid production to stabilize the haloarchaeal cell membrane (Giani and Martinez-Espinosa, 2020). Next, the salinity stresses were investigated with using two different salts, sodium chloride and magnesium sulfate. The highest carotenoid productions (0.145 ± 0.01 A_{490nm} ml^{-1} and 0.208 ± 0.024 A_{490nm} ml^{-1}) were exhibited at the concentration of sodium chloride (20%) and magnesium sulgate (5%), respectively (Fig. 6C and D). In the case of sodium chloride, low concentration brought out cell lysis and more than 25% sodium chloride concentration caused to diminish dissolved oxygen in broth medium and to decrease cell growth and carotenoid production. Besides, it was elucidated that the presence of magnesium ion could support the enhancement of carotenoid production by strain MBLA-0099^T, which could interpreted by the role of magnesium ion as the sophisticated mechanism for haloarchaea to protect the cell against salinity stress (Kellermann *et al*., 2016).

Antibacterial activities of bacterioruberin extracted from strain MBLA0099^T

The antibacterial activity of bacterioruberin was indicated by the formation of clear zones around the discs. Streptomycin (10 μg/ml) showed clear zones of inhibition against all tested pathogens. On the other hand, various concentration of bacterioruberin (2.5–100 μg/ml) resolved in DMSO revealed no zones of inhibition including negative control (data not shown). Although microbial pigements has been reported to possess antimicrobial activity as well as antioxidant property to protect the corresponding microorganisms from various stress conditions (Fariq *et al*., 2019), those inetersted pigements has been limited to prodigiosins and C40 carotenoids (Lapenda *et al*., 2015; Karpiński and Adamczak, 2019). As focusing on C_{50} carotenoids including bacterioru-

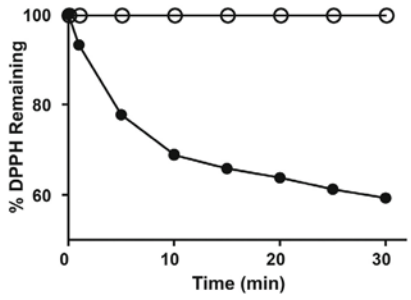

Fig. 7. Time profile of % DPPH free radical remaining. Open and closed circles indicated only DPPH and DPPH with 10 μg/ml bacterioruberin extracted from the strain MBLA0099^T, respectively.

berin and its derivaties from haloarchaea, *Halomonas aquamarina* MB598 was reported to inhibit the growth of some pathogens including *Bacillus cereus*, *Enterococcus faecalis*, and *Klebsiella pneumonia*, of which results are contrast to our results. This different results might be due to the C_{50} carotenoid concentraction used for the agar disk-diffusion method or the specific strains of indicators.

Antioxidant activity of bacterioruberin extracted from the strain MBLA0099^T

DPPH free radical scavenging activity of bacterioruberin extracted from the strain MBLA0099^T was monitored as a function of time (Alvares and Furtado, 2021). The absorbance of only DPPH free radical solution remained unchanged for the reaction. The addition of 10 μg/ml of methanolic bacterioruberin extract to DPPH free radical solution decreased its absorbance at 517 nm. The simultaneous radical scavenging showed 6.7% on addition of bacterioruberin within 1 min, 22.3% at 5 min, 31.1% at 10 min, 34.1% at 15 min, 36.1% at 20 min, 38.7% at 25 min, and 40.7% at 30 min (Fig. 7). After 30 min, the absorbance remained steady-state because of saturation. According to this result, the EC_{50} value of bacterioruberin from strain MBLA0099^T is estimated to be 12.29 μg/ml. A number of studies on DPPH free radical scavenging of bacterioruberin from haloarchaea are reported. The carotenoid extracted from other genus displayed low EC_{50} values (4.81 μg/ml of *Haloferax alexandrinus* and 8.98 μg/ml of *Haloterrigena turkmenica*) compared to strain MBLA0099^T (Hou and Cui, 2018; Alvares and Furtado, 2021). However, it is a low level compared to other commercial antioxidants such as astaxanthin (17.5 μg/ml), BHT (17.2 μg/ml), and ascorbic acid (19.7 μg/ml) (Chintong *et al.*, 2019). These results could suggest that the haloarchaeal carotenoid (especially bacterioruberin) could be considered as an attractive natural antioxidant bioresource.

Conclusion

We isolated one species designated as MBLA0099^T, which represents a novel haloarchaea. Genomic and phylogenetic analyses indicate that strain MBLA0099^T is belonging to the genus *Halorubrum*. Pan-genome analysis shows that strain MBLA0099^T has diverse and distinct strain-specific genes, indicating that strain MBLA0099^T can be distinguished from other previously reported species of the genus *Halorubrum*. Spectrometric and chromatographic analyses show that strain MBLA0099^T produced the red carotenoid bacterioruberin and its precursors. Based on BLAST in the NCBI and KEGG database, the C_{50} carotenoid biosynthesis gene cluster showed that strain MBLA0099^T has similar to other haloarchaeal species already known to produce bacterioruberin. The carotenoid biosynthetic gene information based on the genome of MBLA0099^T revealed that the *crtD* plays a role of bifunctional desaturase activity for the bacterioruberin biosynthesis instead of the *crtI*, even though the crtI-absence which is consistent with other haloarchaeal genomes. Therefore, it should be noted that the gene cluster *crtD-lyeJ-cruF* could be responsible for the bacterioruberin biosynthesis. The strain MBLA0099^T produced relatively high C_{50} carotenoid when its cell culture exposed at the following stresses; netural pH, high oxidative and salinity conditions. Overall genome annotation and analysis of novel haloarchaea species can be encouraged to solve the lack of knowledge about C_{50} carotenoid biosynthesis. Further, haloarchaea has worth of cell factory as a carotenoid producer and C_{50} carotenoid bacterioruberin, which has a strong antioxidant effect, can be applied to functional food resources like C_{40} carotenoid (astaxanthin, zeaxanthin, and lutein) already being sold commercially.

Description of *Halorubrum ruber*

Halorubrum ruber (ru′ber. L. masc. adj. *ruber* red)
Gram-negative, non-motile, rod-shaped having a width of 1.0–1.7 μm and a length of 5.8–6.0 μm. Colonies are red and sticky on ATCC 1176 incubated at 37°C for 7 days. Growth occurs in the 10–45°C (optimum, 37°C) in present of 7.5–30% NaCl (optimum, 17.5%) at pH 5.5–9.0 (optimum, pH 7.0). Growth occurs without Mg^{2+} ion in culture conditions. Casein, gelatin, starch, Tween 20, 40, and 80 hydrolyses are negative. Catalase and oxidase activities are positive and indole production, H_2S formation, dissimilatory nitrate, nitrite reduction, and urease activity are negative. Anaerobic growth does not occur in the presence of DMSO, TMAO, L-arginine, and nitrate. Glycerol, D-galactose, D-glucose, D-fructose, D-mannitol, D-maltose, sucrose, D-raffinose, D-mannose, and D-lactose are utilized as carbon and energy sources. Ampicillin, gentamycin, kanamycin, lincomycin, neomycin, norfloxacin, and streptomycin are susceptible whereas aphidicolin, bacitracin, chloramphenicol, cephalothin, erythromycin, novobiocin, penicillin G, rifampin, and tetracycline are resistant. Major polar lipids are phosphatidylglycerol, phosphatidylglycerol phosphate methyl ester, phosphatidylglycerol sulfate, and sulfated mannosyl glucosyl diether (S-DGD-3). The genome size and G + C content of DNA are 3.02 Mb and 68.9 mol%.

The type strain MBLA0099^T (= KCTC 4296^T = JCM 34701^T) was isolated from seawater of the Yellow Sea near Yeongheung Island. The genome sequence is deposited in GenBank under the accession number CP073695.

Acknowledgements

This work was supported by Incheon National University Research Grant in 2019.

Conflict of Interest

The authors declare that there is no conflict of interest.

References

Alvares, J.J. and Furtado, I.J. 2021. Characterization of multicomponent antioxidants from *Haloferax alexandrinus* GUSF-1 (KF-796625). *3 Biotech* **11**, 58.

Balouiri, M., Sadiki, M., and Ibnsouda, S.K. 2016. Methods for *in vitro* evaluating antimicrobial activity: a review. *J. Pharm. Anal.* **6**, 71–79.

Bauer, A.W., Kirby, M.M., Sherris, J.C., and Truck, M. 1966. Antibiotic susceptibility testing by a standardized single disk method. *Am. J. Clin. Pathol.* **45**, 493–496.

Benson, H.J. 2002. Microbiological Applications: laboratory manual in general microbiology, 8th edn., pp. 432. McGraw-Hill, New York, USA.

Blin, K., Shaw, S., Steinke, K., Villebro, R., Ziemert, N., Lee, S.Y., Medema, M.H., and Weber, T. 2019. antiSMASH 5.0: updates to the secondary metabolite genome mining pipeline. *Nucleic Acids Res.* **47**, W81–W87.

Britton, G. 1995. UV/Visible Spectroscopy. *In* Britton, G., Liaaen-Jensen, S., and Pfander, H. (eds.), Carotenoids, vol. 1B. Birkhäuser Verlag, Basel, Switzerland.

Burns, D.G., Janssen, P.H., Itoh, T., Minegishi, H., Usami, R., Kamekura, M., and Dyall-Smith, M.L. 2010. *Natronomonas moolapensis* sp. nov., non-alkaliphilic isolates recovered from a solar saltern crystallizer pond, and emended description of the genus *Natronomonas*. *Int. J. Syst. Evol. Microbiol.* **60**, 1173–1176.

Capes, M.D., DasSarma, P., and DasSarma, S. 2012. The core and unique proteins of haloarchaea. *BMC Genomics* **13**, 39.

Chaudhari, N.M., Gupta, V.K., and Dutta, C. 2016. BPGA- an ultra-fast pan-genome analysis pipeline. *Sci. Rep.* **6**, 24373.

Chen, L., Yang, J., Yu, J., Yao, Z., Sun, L., Shen, Y., and Jin, Q. 2005. VFDB: a reference database for bacterial virulence factors. *Nucleic Acids Res.* **33**, D325–D328.

Chin, C.S., Alexander, D.H., Marks, P., Klammer, A.A., Drake, J., Heiner, C., Clum, A., Copeland, A., Huddleston, J., Eichler, E.E., *et al.* 2013. Nonhybrid, finished microbial genome assemblies from long-read SMRT sequencing data. *Nat. Methods* **10**, 563–569.

Chintong, S., Phatvej, W., Rerk-Am, U., Waiprib, Y., and Klaypracit, W. 2019. *In vitro* antioxidant, antityrosinase, and cytotoxic activities of astaxanthin from shrimp waste. *Antioxidants* **8**, 128.

Chun, J., Oren, A., Ventosa, A., Christensen, H., Arahal, D.R., da Costa, M.S., Rooney, A.P., Yi, H., Xu, X.W., De Meyer, S., *et al.* 2018. Proposed minimal standards for the use of genome data for the taxonomy of prokaryotes. *Int. J. Syst. Evol. Microbiol.* **68**, 461–466.

Cui, H.L., Zhou, P.J., Oren, A., and Liu, S.J. 2009. Intraspecific polymorphism of 16S rRNA genes in two halophilic archaeal genera, *Haloarcula* and *Halomicrobium*. *Extremophiles* **13**, 31–37.

DasSarma, S. and DasSarma, P. 2017, Halophiles. *In* eLS, John Wiley & Sons, New Jersey, USA.

Edgar, R.C. 2004. MUSCLE: multiple sequence alignment with high accuracy and high throughput. *Nucleic Acids Res.* **32**, 1792–1797.

Fang, C.J., Ku, K.L., Lee, M.H., and Su, N.W. 2010. Influence of nutritive factors on C_{50} carotenoids production by *Haloferax mediterranei* ATCC 33500 with two-stage cultivation. *Bioresour. Technol.* **101**, 6487–6493.

Fariq, A., Yasmin, A., and Jamil, M. 2019. Production, characterization and antimicrobial activities of bio-pigments by *Aquisalibacillus elongatus* MB592, *Salinicoccus sesuvii* MB597, and *Halomonas aquamarina* MB598 isolated from Khewra Salt Range, Pakistan. *Extremophiles* **23**, 435–449.

Feng, J., Zhou, P.J., and Liu, S.J. 2004. *Halorubrum xinjiangense* sp. nov., a novel halophile isolated from saline lakes in China. *Int. J. Syst. Evol. Microbiol.* **54**, 1789–1791.

Felsenstein, J. 1981. Evolutionary trees from DNA sequences: a maximum likelihood approach. *J. Mol. Evol.* **17**, 368–376.

Flores, N., Hoyos, S., Venega, M., Galetović, A., Zúñiga, L.M., Fábrega, F., Paredes, B., Salazar-Ardiles, C., Vilo, C., Ascaso, C., *et al.* 2020. *Haloterrigena* sp. strain SGH1, a bacterioruberin-rich, perchlorate-tolerant halophilic archaeon isolated from halite microbial communities, Atacama Desert, Chile. *Front. Microbiol.* **11**, 324.

Forján, E., Navarro, F., Cuaresma, M., Vaquero, I., Ruíz-Domínguez, M.C., Gojkovic, Ž., Vázquez, M., Márquez, M., Mogedas, B., Bermejo, E., *et al.* 2015. Microalgae: fast-growth sustainable green factories. *Crit. Rev. Environ. Sci. Technol.* **45**, 1705–1755.

Fullmer, M.S., Soucy, S.M., Swithers, K.S., Makkay, A.M., Wheeler, R., Ventosa, A., Gogarten, J.P., and Papke, R.T. 2014. Population and genomic analysis of the genus *Halorubrum*. *Front. Microbiol.* **5**, 140.

Giani, M., Garbayo, I., Vílchez, C., and Martínez-Espinosa, R.M. 2019. Haloarchaeal carotenoids: healthy novel compounds from extreme environments. *Mar. Drugs* **17**, 524.

Giani, M. and Martínez-Espinosa, R.M. 2020. Carotenoid as a protection mechanism against oxidative stress in *Haloferax mediterranei*. *Antioxidant* **9**, 1060.

Giani, M., Miralles-Robledillo, J.M., Peiró, G., Pire, C., and Martinez-Espinosa, R.M. 2020. Deciphering pathway for carotenogenesis in haloarchaea. *Molecules* **25**, 1197.

Gibtan, A., Song, H.S., Kim, J.Y., Kim, Y.B., Park, N., Park, K., Lee, S.J., Kwon, J.K., Roh, S.W., and Lee, H.S. 2018. *Halorubrum aethiopicum* sp. nov., an extremely halophilic archaeon isolated from commercial rock salt. *Int. J. Syst. Evol. Microbiol.* **68**, 416–422.

Gonzalez, C., Gutierrez, and C., Ramirez, C. 1978. *Halobacterium vallismortis* sp. nov. An amylolytic and carbohydrate-metabolizing, extremely halophilic bacterium. *Can. J. Microbiol.* **24**, 710–715.

Hall, T.A. 1999. BioEdit: a user-friendly biological sequence alignment editor and analysis program for Windows 95/98/NT. *Nucleic Acids Symp. Ser.* **41**, 95–98.

Holding, A. and Collee, J. 1971. Chapter I Routine biochemical tests. *Methods Microbiol.* **6**, 1–32.

Hou, J. and Cui, H.L. 2018. *In vitro* antioxidant, antihemolytic, and anticancer activity of the carotenoids from halophilic archaea. *Curr. Microbiol.* **75**, 266–271.

Huerta-Cepas, J., Forslund, K., Coelho, L.P., Szklarczyk, D., Jensen, L.J., von Mering, C., and Bork, P. 2017. Fast genome-wide functional annotation through orthology assignment by eggNOG-Mapper. *Mol. Biol. Evol.* **34**, 2115–2122.

Huerta-Cepas, J., Szklarczyk, D., Heller, D., Hernández-Plaza, A., Forslund, S.K., Cook, H., Mende, D.R., Letunic, I., Rattei, T., Jensen, L.J., *et al.* 2019. eggNOG 5.0: a hierarchical, functionally and phylogenetically annotated orthology resource based on 5090 organisms and 2502 viruses. *Nucleic Acids Res.* **47**, D309–D314.

Kamekura, M., Dyall-smith, M.L., Upasani, V., Ventosa, A., and Kates, M. 1997. Diversity of alkaliphilic halobacteria: proposals for transfer of *Natronobacterium vacuolatum*, *Natronoba cteriummagadii*, and *Natronobacterium pharaonis* to *Halorubrum*, *Natrialba*, and *Natronomonas* gen. nov., respectively, as *Halorubrum vacuolatum* comb. nov., *Natrialba magadii* comb. nov., and *Natronomonas pharaonis* comb. nov., respectively. *Int. J. Syst. Evol. Microbiol.* **47**, 853–857.

Kanehisa, M. and Goto, S. 2000. KEGG: Kyoto encyclopedia of genes and genomes. *Nucleic Acids Res.* **28**, 27–30.

Karpiński, T. and Adamczak, A. 2019. Fucoxanthin - an antibacterial carotenoid. *Antioxidants* **8**, 239.

Kellermann, M.Y., Yoshinaga, M.Y., Valentine, R.C., Wörmer, L., and Valentine, D.L. 2016. Important roles for membrane lipids in haloarchaeal bioenergetics. *Biochim. Biophys. Acta Biomembr.* **1858**, 2940–2956.

Kharroub, K., Quesada, T., Ferrer, R., Fuentes, S., Aguilera, M., Boulahrouf, A., Ramos-Cormenzana, A., and Monteoliva-Sánchez, M. 2006. *Halorubrum ezzemoulense* sp. nov., a halophilic archaeon isolated from Ezzemoul sabkha, Algeria. *Int. J. Syst. Evol. Microbiol.* **56**, 1583–1588.

Kim, D., Park, S., and Chun, J. 2021. Introducing EzAAI: a pipeline for high throughput calculations of prokaryotic average amino acid identity. *J. Microbiol.* **59**, 476–480.

Kimura, M. 1980. A simple method for estimating evolutionary rates of base substitutions through comparative studies of nucleotide sequences. *J. Mol. Evol.* **16**, 111–120.

Kluge, A.G. and Farris, J.S. 1969. Quantitative phyletics and the evolution of anurans. *Syst. Biol.* **18**, 1–32.

Konstantinidis, K.T. and Tiedje J.M. 2005. Towards a genome-based taxonomy for prokaryotes. *J. Bacteriol.* **187**, 6258–6264.

Kumar, S., Stecher, G., and Tamura, K. 2016. MEGA7: molecular evolutionary genetics analysis version 7.0 for bigger datasets. *Mol. Biol. Evol.* **33**, 1870–1874.

Lapenda, J.C., Silva, P.A., Vicalvi, M.C., Sena, K.X.F.R., and Nascimento, S.C. 2015. Antimicrobial activity of prodigiosin isolated from *Serratia marcescens* UFPEDA 398. *World J. Microbiol. Biotechnol.* **31**, 399–406.

Lee, I., Kim, Y.O., Park, S.C., and Chun, J. 2016. OrthoANI: an improved algorithm and software for calculating average nucleotide identity. *Int. J. Syst. Evol. Microbiol.* **66**, 1100–1103.

Lee, I., Chalita, M., Ha, S.M., Na, S.I., Yoon, S.H., and Chun, J. 2017. ContEst16S: an algorithm that identifies contaminated prokaryotic genomes using 16S RNA gene sequences. *Int. J. Syst. Evol. Microbiol,* **67**, 2053–2057.

Liaaen-Jensen, S., Hertzberg, S., Weeks, O.B., and Schwieter, U. 1968. Bacterial carotenoids XXVII. C50-carotenoids. 3. Structure determination of dehydrogenans-P439. *Acta Chem. Scand.* **22**, 1171–1186.

McGenity, T.J. and Grant, W.D. 1995. Transfer of *Halobacterium saccharovorum*, *Halobacterium sodomense*, *Halobacterium trapanicum* NRC 34021 and *Halobacterium lacusprofundi* to the genus *Halorubrum* gen. nov., as *Halorubrum saccharovorum* comb. nov., *Halorubrum sodomense* comb. nov., *Halorubrum trapanicum* comb. nov., and *Halorubrum lacusprofundi* comb. nov. *Syst. Appl. Microbiol.* **18**, 237–243.

McGenity, T.J. and Grant, W.D. 2015. *Halorubrum. In* Trujillo, M.E., Dedysh, S., DeVos, P., Hedlund, B., Kämpfer, P., Rainey, F.A., and Whitman, W.B. (ed), Bergey's Manual of Systematics of Archaea and Bacteria, 2nd edn. John Wiley & Sons, New Jersey, USA.

Meier-Kolthoff, J.P., Auch, A.F., Klenk, H.P., and Göker, M. 2013. Genome sequence-based species delimitation with confidence intervals and improved distance functions. *BMC Bioinformatics* **14**, 60.

Minnikin, D.E., O'Donnell, A.G., and Goodfellow, M. 1984. An integrated procedure for the extraction of bacterial isoprenoid quinones and polar lipids. *J. Microbiol. Methods.* **2**, 233–241.

Montero-Lobato, Z., Ramos-Merchanete, A., Fuentes, J.L., Sayago, A., Fernández-Recamales, Á., Martínez-Espinosa, R.M., Vega, J.M., Vílchez, C., and Garbayo, I. 2018. Optimization of growth and carotenoid production by *Haloferax mediterranei* using response surface methodology. *Mar. Drugs* **16**, 372.

Nakano, T. and Wiegertjes, G. 2020. Properties of carotenoids in fish fitness: a review. *Mar. Drugs* **18**, 568.

Oren, A. and Rodríguez-Valera, F. 2001. The contribution of halophilic Bacteria to the red coloration of saltern crystallizer ponds[1]. *FEMS Microbiol. Ecol.* **36**, 123–130.

Paliwal, C., Mitra, M., Bhayani, K., Bharadwaj, S.V.V., Ghosh, T., Dubey, S., and Mishra, S. 2017. Abiotic stresses as tools for metabolites in microalgae. *Bioresour. Technol.* **244**, 1216–1226.

Pesenti, P.T., Sikaroodi, N., Gillevet, P.M., Sánchez-Porro, C., Ventosa, A., and Litchfield, C.D. 2008. *Halorubrum californiense* sp. nov., an extreme archaeal halophile isolated from a crystallizer pond at a solar salt plant in California, USA. *Int. J. Syst. Evol. Microbiol.* **58**, 2710–2715.

Saitou, N. and Nei, M. 1987. The neighbor-joining method: a new method for reconstructing phylogenetic trees. *Mol. Biol. Evol.* **4**, 406–425.

Serrano, S., Mendo, S., and Caetano, T. 2021. Haloarchaea have a high genomic diversity for the biosynthesis of carotenoids of biotechnological interest. *Res. Microbiol.* **20**, 103919.

Shahmohammadi, H.R., Asgarani, E., Terato, H., Saito, T., Ohyama, Y., Gekko, K., Yamamoto, O., and Ide, H. 1998. Protective roles of bacterioruberin and intracellular KCl in the resistance of *Halobacterium salinarium* against DNA-damaging agents. *J. Radiat. Res.* **39**, 251–262.

Smibert, R.M. and Krieg, N.R. 1994. Phenotypic characterization. *In* Gerhart, P., Murray, R.G.E., Wood, W.A., and Krieg, N.R. (eds.) Methods for General and Molecular Bacteriology, pp. 607–654. American Society for Microbiology, Washington DC, USA.

Thombre, R.S., Shinde, V.D., Oke, R.S., Dhar, S.K., and Shouche, Y.S. 2016. Biology and survival of extremely halophilic archaeon *Haloarcula marismortui* RR12 isolated from Mumbai salterns, India in response to salinity stress. *Sci. Rep.* **6**, 25642.

Tittsler, R.P. and Sandholzer, L.A. 1936. The use of semi-solid agar for the detection of bacterial motility. *J. Bacteriol.* **31**, 575–580.

Ventosa, M., Gutiérrez, M.C., Kamekura, M., Zvyagintseva, I.S., and Oren, A. 2004. Taxonomic study of *Halorubrum distributum* and proposal of *Halorubrum terrestre* sp. nov. *Int. J. Syst. Evol. Microbiol.* **54**, 389–392.

Yang, Y., Yatsunami, R., Ando, A., Miyoko, N., Fukui, T., Takaichi, S., and Nakamura, S. 2015. Complete biosynthetic pathway of the C_{50} carotenoid bacterioruberin from lycopene in the extremely halophilic archaeon *Haloarcula japonica*. *J. Bacteriol.* **197**, 1614–1623.

Yatsunami, R., Ando, A., Yang, Y., Takaichi, S., Kohno, M., Matsumura, Y., Ikeda, H., Fukui, T., Nakasone, K., Fujita, N., *et al.* 2014. Identification of carotenoids from the extremely halophilic archaeon *Haloarcula japonica*. *Front. Microbiol.* **5**, 100.

Zhao, Y., Wu, J., Yang, J., Sun, S., Xiao, J., and Yu, J. 2012. PGAP: pan-genomes analysis pipeline. *Bioinformatics* **28**, 416–418.